

## Universality in the atom-exchange reaction involving Feshbach molecules

Jue Nan, Ya-Xiong Liu, De-Chao Zhang , Lan Liu, Huan Yang , Bo Zhao, and Jian-Wei Pan

*Hefei National Laboratory for Physical Sciences at Microscale and Department of Modern Physics, University of Science and Technology of China, Hefei, Anhui 230026, China*

*and Shanghai Branch, CAS Center for Excellence and Synergetic Innovation Center in Quantum Information and Quantum Physics, University of Science and Technology of China, Shanghai 201315, China*



(Received 14 October 2019; published 6 December 2019)

We study the atom-exchange reaction involving Feshbach molecules in the overlapping Feshbach resonance at about 106.8 G in the  $^{23}\text{Na}^{40}\text{K}$  system. We measure the reaction-rate coefficients as a function of the magnetic field in the exothermic regime. The measured reaction-rate coefficients in the current work and the reaction-rate coefficients measured in the previous work [Phys. Rev. A **100**, 032706 (2019)] in the vicinity of the overlapping Feshbach resonance at a magnetic field of about 130 G can be quantitatively explained by a universal model using the three-body parameter. Our results indicate that the universality might exist in the atom-exchange reaction involving Feshbach molecules.

DOI: [10.1103/PhysRevA.100.062704](https://doi.org/10.1103/PhysRevA.100.062704)

Ultracold atoms with magnetically tunable Feshbach resonances offer great opportunities to study few-body physics with resonant two-body interactions [1–3]. One of the well-known examples is the observation of the three-body Efimov resonance, whose existence has been debated in theory for several decades. In an ultracold atomic gas, the Efimov bound state manifests itself as a resonant enhancement of the three-body recombination or the atom-dimer relaxation [4–8]. Besides the large two-body scattering length, precisely describing the Efimov physics requires a three-body parameter, which accounts for the short-range physics. In an ultracold atomic gas, the three-body parameter exhibits the universal behavior, i.e., the three-body parameters in different atomic systems are almost universally related to the long-range van der Waals interaction between the atoms. This kind of universality was first observed in an ultracold Cs gas by studying the three-body recombination in the vicinity of several different broad Feshbach resonances of the same spin state [9]. It was also observed in  $^7\text{Li}$  and  $^{39}\text{K}$  gases that the three-body parameter is essentially independent of the hyperfine or the nuclear-spin state [10,11]. The origin of the universality was later interpreted as the van der Waals universality, which is caused by a repulsive barrier due to the long-range van der Waals potential [12–14]. This kind of universality is also observed in studying the resonantly enhanced atom-dimer relaxation [15,16].

In the vicinity of overlapping Feshbach resonances, where the binding energies of different Feshbach molecules intersect at a certain magnetic field, a new kind of three-body problem, the atom-exchange reaction between an atom and a Feshbach molecule, can be studied [17]. Such an atom-exchange process is also modified by the presence of the Efimov state. Therefore, a natural and important question is whether universal properties also exist in the atom-exchange reaction. In Ref. [18], the atom-exchange-rate coefficient of the  $A_2 + B \rightarrow AB + A$  collision is enhanced when the reaction is energetically favorable, where  $A$  and  $B$  are different

hyperfine states of the Cs atom. The enhancement is observed in two different collision channels, which indicates the existence of the universality. However, the theoretical model only provides a qualitative description to the experiments. In Ref. [19], the reaction-rate coefficient of the  $|12\rangle + |3\rangle \rightarrow |23\rangle + |1\rangle$  collision is suppressed when the reaction is energetically favorable, where  $|1\rangle$ ,  $|2\rangle$ , and  $|3\rangle$  represent different hyperfine states of the  $^6\text{Li}$  atom. The loss minimum is observed at two different magnetic fields in the same collision channel. In Ref. [20] the authors use a universal model to quantitatively compare theory with experiment. They find that the theoretically calculated locations of the minima deviate from the experiment, which is partially due to the fact that only the overall loss rate rather than the reaction rate is measured.

There are two overlapping Feshbach resonances between  $^{23}\text{Na}$  and  $^{40}\text{K}$  atoms. The Feshbach resonance between the  $|f, m_f\rangle_{\text{Na}} = |1, 1\rangle$  and  $|f, m_f\rangle_{\text{K}} = |9/2, -5/2\rangle$  states at about 138 G and the Feshbach resonance between the  $|1, 1\rangle$  and  $|9/2, -3/2\rangle$  states at 130.7 G overlap at about 130.24 G. The resonance strength parameters for these two resonances are  $s_{\text{res}} = 14.6$  and  $s_{\text{res}} = 0.38$ , respectively [21]. In our previous works [22,23], we have studied the state-to-state reaction dynamics in the vicinity of this overlapping Feshbach resonance in detail and obtained the three-body parameter by comparing theory with experiment. In this paper, we study the reaction dynamics of the same mixture close to another overlapping Feshbach resonance located at about 106.8 G, where the Feshbach resonance between the  $|1, 1\rangle$  and  $|9/2, -7/2\rangle$  states at about 110 G and the Feshbach resonance between the  $|1, 1\rangle$  and  $|9/2, -5/2\rangle$  states at about 107 G overlap. The resonance strength parameters for these two resonances are  $s_{\text{res}} = 12.3$  and  $s_{\text{res}} = 0.43$ , respectively [21]. This overlapping Feshbach resonance provides the opportunity to study the universal properties of the atom-exchange reaction. One advantage in the  $^{23}\text{Na}^{40}\text{K}$  system is that the distinguishability of the two internal states of the  $^{40}\text{K}$  atom can be employed

to study the state-to-state reaction dynamics, and thus we can directly compare theory with experiment.

In our experiment, the ultracold atomic mixture is prepared by first loading  $^{23}\text{Na}$  and  $^{40}\text{K}$  atoms into a two-species dark-spot magneto-optical trap (MOT) via a Zeeman slower and a two-dimensional (2D) MOT, respectively. The atoms are then transferred to a magnetic trap to perform evaporative cooling of  $^{23}\text{Na}$  atoms, and  $^{40}\text{K}$  atoms are sympathetically cooled. The atomic mixture is transferred to an crossed-beam optical dipole trap with a wavelength of 1064 nm and further cooled. We typically prepare  $3 \times 10^5$   $^{23}\text{Na}$  atoms and  $1.6 \times 10^5$   $^{40}\text{K}$  atoms at a temperature of about 600 nK. The ultracold atomic mixture is confined in the optical dipole trap with the trap frequencies along the three Cartesian coordinate axes for  $^{40}\text{K}$  being  $2\pi \times (250, 237, 79)$  Hz. The  $^{23}\text{Na}$  atoms are prepared in the  $|1, 1\rangle$  state, and the  $^{40}\text{K}$  atoms can be prepared in a certain hyperfine state by a Landau-Zener transfer. In our experiment, the magnetic field is actively stabilized and the uncertainty is about 10 mG.

The Feshbach resonance between  $|1, 1\rangle$  and  $|9/2, -7/2\rangle$  at about 110 G and the Feshbach resonance between  $|1, 1\rangle$  and  $|9/2, -5/2\rangle$  at about 107 G were observed in Ref. [24] by measuring the atom loss as a function of magnetic field. To precisely characterize the Feshbach resonances in these collision channels, we measure the binding energies of the Feshbach molecules by performing rf loss spectroscopy [22,25]. To this end, we apply a long, weak rf pulse to the atomic mixture at a certain magnetic field close to the atomic Feshbach resonance and observe the atom losses as a function of the rf frequency. The binding energy is extracted from the rf loss spectrum by using the model introduced in Refs. [22,25]. The measured binding energies of the Feshbach molecules in the two collision channels are shown in Fig. 1. The binding energies are fit by using the universal model  $E^b = \hbar^2 / \{2\mu_d [\tilde{a}(B) - \tilde{a}]^2\}$ , where  $\mu_d = m_A m_B / (m_A + m_B)$  is the reduced mass and  $\tilde{a} = 2\pi(2\mu_d C_6 / \hbar^2)^{1/4} / \Gamma(1/4)^2 \approx 51a_0$  is the mean scattering length, with  $a_0$  and  $C_6$  being the Bohr radius and the van der Waals constant between  $^{23}\text{Na}$  and  $^{40}\text{K}$ , respectively. The scattering length near a Feshbach resonance can be expressed as a function of magnetic field,  $\tilde{a}(B) = a_{\text{bg}} [1 - \Delta B / (B - B_0)]$ , where  $a_{\text{bg}}$  is the background scattering length, and  $B_0$  and  $\Delta B$  are the position and width of the Feshbach resonance, respectively. For the Feshbach resonance between  $|1, 1\rangle$  and  $|9/2, -7/2\rangle$ , we obtain the parameters  $a_{\text{bg}} = -550(25)a_0$ ,  $B_0 = 110.31(19)$  G, and  $\Delta B = -21.1(1)$  G. For the Feshbach resonance between  $|1, 1\rangle$  and  $|9/2, -5/2\rangle$ , we obtain  $a_{\text{bg}} = 98(5)a_0$ ,  $B_0 = 107.02(1)$  G, and  $\Delta B = 5.5(4)$  G. It can be readily seen that the two Feshbach resonances intersect at  $B_{\text{th}} = 106.82$  G.

We study the atom-exchange reaction of the type  $AB + C \rightarrow AC + B$ , where  $A$  represents the  $|1, 1\rangle$  state of  $^{23}\text{Na}$ ,  $B$  and  $C$  represent the  $|9/2, -7/2\rangle$  and  $|9/2, -5/2\rangle$  states of  $^{40}\text{K}$ , and  $AB$  and  $AC$  denote the Feshbach molecules. The energy released in the reaction is plotted as a function of magnetic field in Fig. 1(b). It can be clearly seen that the reaction is exothermic at  $B < B_{\text{th}}$  and endothermic at  $B > B_{\text{th}}$ . To fully study the reaction dynamics, the energy released in the reaction has to be small enough so that the reaction products can still be trapped and detected. Therefore, in principle we could study the reaction for magnetic fields

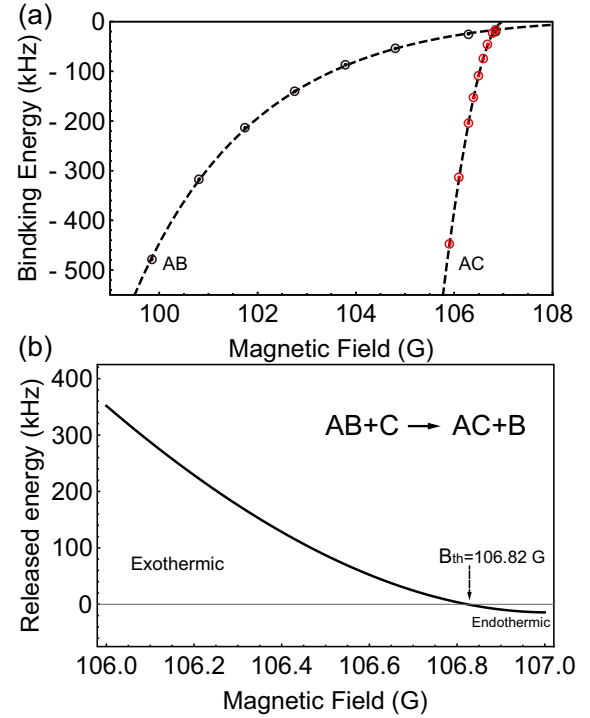


FIG. 1. (a) Characterization of the overlapping Feshbach resonance. The measured binding energies of the  $AB$  and  $AC$  Feshbach molecules are plotted as a function of magnetic field. The dashed lines are the fits of the data points using the universal model. (b) The energy  $\Delta E$  released in the  $AB + C \rightarrow AC + B$  atom-exchange reaction is plotted as a function of magnetic field in the range of 106–107 G.  $\Delta E$  is zero at  $B_{\text{th}} = 106.82$  G. At magnetic fields lower than  $B_{\text{th}}$ , the reaction is exothermic and thus energetically favorable. At magnetic fields higher than  $B_{\text{th}}$ , the reaction is endothermic. Error bars represent  $\pm 1$  standard deviation.

larger than about 106.1 G. However, for magnetic fields larger than 106.82 G, where the reaction is endothermic, the binding energy of the  $AC$  molecule is smaller than 10 kHz. For such a small binding energy, it is difficult to prepare the  $AC$  molecule without transferring the atom to the  $C$  state by using the Raman photoassociation method. Therefore, in this work, we only study the exothermic reaction in the magnetic-field range of 106.1–106.82 G.

To study the atom-exchange reaction, we prepare the atom-dimer mixture  $AB + C$  as follows: For magnetic fields smaller than about 106.3 G, we can directly associate the  $AB$  molecules from the  $A + C$  atomic mixture by employing the Raman photo-association method [26,27]. The Raman lasers couple the  $B$  and  $C$  states, with a blue detuning of about 250 GHz relative to the  $D_2$  line of  $^{40}\text{K}$ . The two beams are derived from the same laser and the frequency difference is close to the frequency difference between the  $AB$  bound state and the  $A + C$  free atomic state. The Rabi frequency for the atomic transition is about 90 kHz. We use a Gaussian shape pulse with a duration of about 300  $\mu\text{s}$  to suppress the sideband.

For magnetic fields between 106.3 and 106.82 G, the association of the  $AB$  molecules from the  $A + C$  mixture is not favorable. This is because the presence of a bound state in the collision channel between  $A$  and  $C$  suppresses the bound-free

Franck-Condon coefficient, and thus the association efficiency is largely reduced [28]. To solve this problem, we employ the indirect preparation method developed in our previous work [23]. We start from the  $A + |9/2, -3/2\rangle$  mixture and associate the  $AC$  molecule by using Raman photo-association, and then transfer the  $AC$  molecule to the  $AB$  molecule by applying a bound-bound rf  $\pi$  pulse. After that, we transfer the remaining atoms in the  $|9/2, -3/2\rangle$  state to the  $C$  state by another  $\pi$  pulse. In this way, the  $AB + C$  mixture is prepared.

To study the reaction dynamics, after the reactants are prepared, we monitor the time evolution of the  $AB$  molecule and of the  $B$  atom product. The  $AB$  molecule is detected by applying a rf pulse to dissociate the  $AB$  molecule into the  $A + |9/2, -9/2\rangle$  state and then detecting the atom in the  $|9/2, -9/2\rangle$  state. The frequency of the dissociation pulse is chosen to be about 70 kHz larger than the binding energy of the  $AB$  molecule and its pulse length is about 0.5 ms, so that the  $AB$  molecules can be fully dissociated. To detect the  $B$  atom, we apply a  $\pi$  pulse of about 70  $\mu$ s to resonantly transfer the  $B$  atom to the  $|9/2, -9/2\rangle$  state for detection. The atoms and the molecules are measured in separate experiments by repeating the same preparation sequences.

The time evolutions of the  $AB$  molecule and the  $B$  atom numbers at different magnetic fields are plotted in Fig. 2. The time evolutions are fit by using exponential functions. The reaction-rate coefficient is given by [23]

$$\beta_r = \frac{\dot{N}_B(0)}{\bar{n}_C N_{AB}(0)}, \quad (1)$$

where  $N_{AB}(0)$  is the number of  $AB$  molecules at  $t = 0$ , and  $\dot{N}_B(0)$  is the derivative of the time evolution of the number of  $B$  atoms at  $t = 0$ . These two parameters are obtained from the exponential fits to the data points. Note that, when calculating the reaction-rate coefficients, the molecule number has been corrected by taking into account the long dissociation pulse using the method discussed in Ref. [22]. The mean density of the  $C$  atoms is calculated by  $\bar{n}_C = \alpha N_C$ , with  $\alpha = [(m_K \bar{\omega}^2)/(4\pi k_B T)]^{3/2}$ , where  $T$  is the temperature and  $\bar{\omega}$  represents the geometric mean of the trap frequencies. We have assumed that the mean density  $\bar{n}_C$  can be approximated by a time-independent constant, since the number of the  $C$  atoms is much greater than the number of the  $AB$  molecules.

At  $B = B_{th}$ , the binding energy of the  $AB$  molecule is about 16 kHz. This is comparable to the kinetic energy  $k_B T \simeq h \times 12$  kHz with  $k_B$  being the Boltzmann constant and  $T = 600$  nK. Therefore, at magnetic fields very close to 106.82 G, thermal collisions may cause dissociations of the  $AB$  molecules into  $A + B$  free atoms. This may affect the study of the reaction dynamics, since we cannot distinguish whether the  $B$  atoms are created by the atom-exchange reaction or by thermal collisions. We estimate the contributions from the collision-induced dissociation as follows: Assuming that the collision dissociation is only caused by thermal collision and is thus independent of the hyperfine state, we estimate the collisional dissociation rate by preparing the  $AB + |9/2, -3/2\rangle$  mixture at magnetic fields close to 106.82 G and then measuring the decay of  $AB$  molecules and the increase of the  $B$  atom number. We find that the collision dissociation rate is about one order of magnitude smaller than the reaction-rate

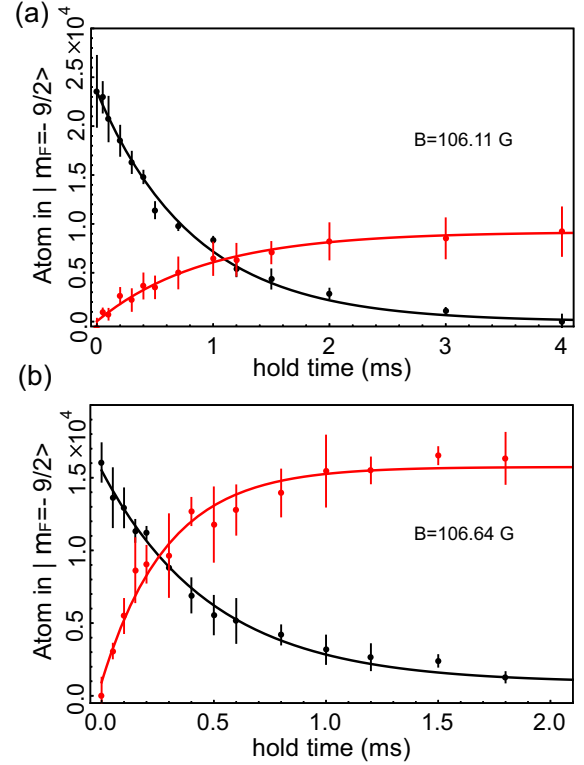


FIG. 2. The time evolutions of the  $AB$  molecular reactant and the  $B$  atomic product at different magnetic fields. The black solid lines and the red (light-gray) solid lines are exponential fits to the data points, respectively. (a) The data points are measured at  $B = 106.11$  G, where the  $AB$  molecules are associated from the  $A + C$  mixture. The  $1/e$  time constants are  $\tau_{AB} = 0.84 \pm 0.06$  ms and  $\tau_B = 0.93 \pm 0.10$  ms, respectively. (b) The data points are measured at  $B = 106.64$  G, where the  $AB$  molecules are prepared by the indirect method based on the molecular bound-bound transition. The  $1/e$  time constants are  $\tau_{AB} = 0.50 \pm 0.04$  ms and  $\tau_B = 0.29 \pm 0.04$  ms, respectively. Error bars represent  $\pm 1$  standard deviation.

coefficient. Therefore, we neglect the contribution due to the collision dissociation in the following discussions.

The measured reaction-rate coefficients in the magnetic-field range from 106.1 to 106.81 G are plotted in Fig. 3 as a function of the magnetic field. It can be readily seen that the reaction-rate coefficient is enhanced when the energy released in the reaction decreases. This is qualitatively consistent with our previous experiment [22,23]. To quantitatively understand the reaction-rate coefficients, we calculate the reactive scattering amplitude by solving the universal zero-range Skorniakov-Ter Martirosian (STM) equations [1,29–31]

$$t_{ii}(k, p, E) = \frac{m_A}{\pi \mu_d} \sqrt{\frac{a_{AC}}{a_{AB}}} \int^\Lambda dq \frac{q}{2k} K(k, q, E) \times D_{AC}(q, E) t_{\bar{i}\bar{i}}(q, p, E), \quad (2)$$

$$t_{\bar{i}\bar{i}}(k, p, E) = \frac{2\pi \hbar^4}{\mu_d^2 \sqrt{a_{AB} a_{AC}}} \frac{m_A}{2pk} K(k, p, E) + \frac{m_A}{\pi \mu_d} \sqrt{\frac{a_{AB}}{a_{AC}}} \int^\Lambda dq \frac{q}{2k} K(k, q, E) \times D_{AB}(q, E) t_{ii}(q, p, E), \quad (3)$$

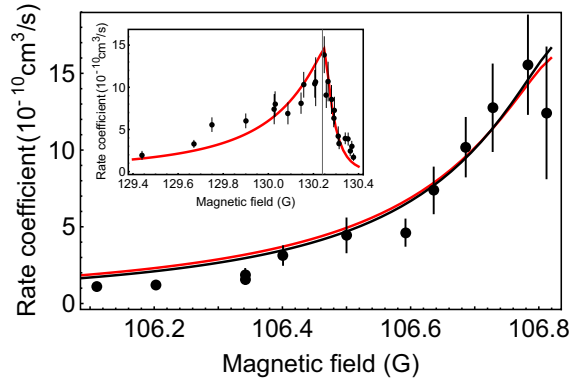


FIG. 3. Measured rate coefficients as a function of magnetic field. The black solid line is a fit to the data with the fitting parameter  $\ln(\Lambda a_0) = 2.28 \pm 0.40$  and the normalization coefficient  $C_\beta = 2.35 \pm 0.31$ . The red (light-gray) solid line is a fit using the theoretical calculations to the data points in the current work and in our previous work in the vicinity of 130 G, using a single dimensionless three-body parameter. The dimensionless three-body parameter determined in this way is  $\ln(\Lambda a_0) = 2.42 \pm 0.39$ . The inset shows the fittings to the data points at about 130 G. Error bars represent  $\pm 1$  standard deviation.

where

$$K(k, p, E) = \ln \frac{2\mu_d E - p^2 - k^2 + 2\mu_d p k / m_A}{2\mu_d E - p^2 - k^2 - 2\mu_d p k / m_A}, \quad (4)$$

$$D_{AB,AC}(q, E) = \left[ -\frac{\hbar}{a_{AB,AC}} + \sqrt{-2\mu_d \left( E - \frac{q^2}{2\mu_{ad}} \right)} \right]^{-1}. \quad (5)$$

Here channel  $i$  denotes the entrance channel  $AB + C$ , and channel  $f$  denotes the reaction channel  $AC + B$ . The elastic and reactive scattering amplitudes are given by  $t_{ii}(k, p, E)$  and  $t_{if}(k, p, E)$ , where  $p$  and  $k$  are the relative momenta between the atom and the molecule in the incoming and outgoing channels, respectively,  $E$  is the total energy, and  $\mu_{ad} = m_A(m_A + m_B)/(2m_A + m_B)$  is the reduced mass of the atom and molecule. The two-body scattering lengths in the two channels are  $a_{AB}$  and  $a_{AC}$ , respectively, and  $\Lambda$  is the three-body parameter.

The reactive scattering amplitude  $t_{if}(k_f, p_i, E)$  is numerically calculated by using the techniques discussed in Ref. [30]. The total collision cross section is given by  $\sigma_r(p_i) = (8\pi^3/h^4)\mu_{ad}^2(k_f/p_i)|t_{if}(k_f, p_i, E)|^2$ . The collision-rate coefficient is thus calculated by  $\beta_r = \int v \sigma_r(v) f(v) dv$ , where we have  $v = p/\mu_{ad}$  and  $f(v) = 4\pi v^2 [\mu_{ad}/(2\pi k_B T)]^{3/2} \exp[-(\mu_{ad} v^2)/(2k_B T)]$  is the Maxwell-Boltzmann distribution.

The calculated reaction-rate coefficients are fit to the data points, where the dimensionless three-body parameter

$\ln(\Lambda a_0)$  and a normalization factor  $C_n$  are the fitting parameters. We obtain  $\ln(\Lambda a_0) = 2.28 \pm 0.40$  and  $C_n = 2.35 \pm 0.31$ . In our previous work studying the atom-exchange process in the vicinity of 130 G [23], we obtain the dimensionless three-body parameter  $\ln(\Lambda a_0) = 3.12$ . The reaction-rate coefficient is a periodic function of the dimensionless three-body parameter  $\ln(\Lambda a_0)$  with a period of about 5.44 [17]. Therefore, the difference between these two parameters  $\ln(\Lambda a_0)$  is about 1/7 of a period. This indicates that a single three-body parameter may be applicable to both overlapping Feshbach resonances. Therefore, we fit the theoretical calculations to the reaction-rate coefficients measured in the current work and in our previous work in the vicinity of 130 G, using a single dimensionless three-body parameter and two normalization factors as the fitting parameters. The dimensionless three-body parameter determined in this way is  $\ln(\Lambda a_0) = 2.42 \pm 0.39$ . The results are shown in Fig. 3. Considering the uncertainties of the data points, the agreement between theory and experiment is good. These results indicate that the same three-body parameter may describe the atom-exchange reaction at two different overlapping Feshbach resonances, and thus the universality might also exist in the atom-exchange reaction involving Feshbach molecules.

In conclusion, we have studied the universality of the atom-exchange reaction in the vicinity of the overlapping Feshbach resonances in the  $^{23}\text{Na}^{40}\text{K}$  system. Our results suggest that the atom-exchange reaction at the two overlapping Feshbach resonances may be explained by the same three-body parameter. It is interesting to compare our system with the  $^6\text{Li}-^{133}\text{Cs}$  system [7], where the van der Waals universality has been carefully studied. In the Li-Cs-Cs system, the two Cs atoms are in the same internal state. It is a ABB system, where Efimov resonances have been directly observed. While in our system, the two  $^{40}\text{K}$  atoms are in different internal states. It is an ABC system and thus the atom-exchange process can be detected. In the  $^6\text{Li}-^{133}\text{Cs}$  system, the Efimov resonances can be calculated from a single-channel scattering model by using only two-body van der Waals interactions [7,12–14]. However, this type of calculation has not been performed to study the atom-exchange process. Our experiments suggest that a similar universality may also exist in the atom-exchange process involving Feshbach molecules. Understanding the universality in atom-exchange processes may require a two-channel scattering model that can account not only for the potential-energy curve but also for the exchange force.

We would like to thank Cheng Chin for stimulating discussions. This work was supported by the National Key R&D Program of China (under Grant No. 2018YFA0306502), the National Natural Science Foundation of China (under Grants No. 11521063 and No. 11904355), the Chinese Academy of Sciences, and the Anhui Initiative in Quantum Information Technologies.

[1] E. Braaten and H.-W. Hammer, *Phys. Rep.* **428**, 259 (2006).

[2] P. Naidon and S. Endo, *Rep. Prog. Phys.* **80**, 056001 (2017).

[3] C. H. Greene, P. Giannakeas, and J. Pérez-Ríos, *Rev. Mod. Phys.* **89**, 035006 (2017).

- [4] T. Kraemer, M. Mark, P. Waldburger, J. G. Danzl, C. Chin, B. Engeser, A. D. Lange, K. Pilch, A. Jaakkola, H.-C. Nägerl *et al.*, *Nature (London)* **440**, 315 (2006).
- [5] M. Zaccanti, B. Deissler, C. D'Errico, M. Fattori, M. Jonas-Lasinio, S. Mueller, G. Roati, M. Inguscio, and G. Modugno, *Nat. Phys.* **5**, 586 (2009).
- [6] S. Knoop, F. Ferlaino, M. Mark, M. Berninger, H. Schöbel, H.-C. Nägerl, and R. Grimm, *Nat. Phys.* **5**, 227 (2009).
- [7] R. Pires, J. Ulmanis, S. Häfner, M. Repp, A. Arias, E. D. Kuhnle, and M. Weidemüller, *Phys. Rev. Lett.* **112**, 250404 (2014).
- [8] S.-K. Tung, K. Jiménez-García, J. Johansen, C. V. Parker, and C. Chin, *Phys. Rev. Lett.* **113**, 240402 (2014).
- [9] M. Berninger, A. Zenesini, B. Huang, W. Harm, H.-C. Nägerl, F. Ferlaino, R. Grimm, P. S. Julienne, and J. M. Hutson, *Phys. Rev. Lett.* **107**, 120401 (2011).
- [10] N. Gross, Z. Shotan, S. Kokkelmans, and L. Khaykovich, *Phys. Rev. Lett.* **105**, 103203 (2010).
- [11] S. Roy, M. Landini, A. Trenkwalder, G. Semeghini, G. Spagnolli, A. Simoni, M. Fattori, M. Inguscio, and G. Modugno, *Phys. Rev. Lett.* **111**, 053202 (2013).
- [12] J. Wang, J. P. D'Incao, B. D. Esry, and C. H. Greene, *Phys. Rev. Lett.* **108**, 263001 (2012).
- [13] Y. Wang, J. Wang, J. P. D'Incao, and C. H. Greene, *Phys. Rev. Lett.* **109**, 243201 (2012).
- [14] P. Naidon, S. Endo, and M. Ueda, *Phys. Rev. A* **90**, 022106 (2014).
- [15] R. S. Bloom, M.-G. Hu, T. D. Cumby, and D. S. Jin, *Phys. Rev. Lett.* **111**, 105301 (2013).
- [16] K. Kato, Y. Wang, J. Kobayashi, P. S. Julienne, and S. Inouye, *Phys. Rev. Lett.* **118**, 163401 (2017).
- [17] J. P. D'Incao and B. D. Esry, *Phys. Rev. Lett.* **103**, 083202 (2009).
- [18] S. Knoop, F. Ferlaino, M. Berninger, M. Mark, H.-C. Nägerl, R. Grimm, J. P. D'Incao, and B. D. Esry, *Phys. Rev. Lett.* **104**, 053201 (2010).
- [19] T. Lompe, T. B. Ottenstein, F. Serwane, K. Viering, A. N. Wenz, G. Zürn, and S. Jochim, *Phys. Rev. Lett.* **105**, 103201 (2010).
- [20] H.-W. Hammer, D. Kang, and L. Platter, *Phys. Rev. A* **82**, 022715 (2010).
- [21] A. Viel and A. Simoni, *Phys. Rev. A* **93**, 042701 (2016).
- [22] J. Rui, H. Yang, L. Liu, D.-C. Zhang, Y.-X. Liu, J. Nan, Y.-A. Chen, B. Zhao, and J.-W. Pan, *Nat. Phys.* **13**, 699 (2017).
- [23] Y.-X. Liu, J. Nan, D.-C. Zhang, L. Liu, H. Yang, J. Rui, B. Zhao, and J.-W. Pan, *Phys. Rev. A* **100**, 032706 (2019).
- [24] J. W. Park, C.-H. Wu, I. Santiago, T. G. Tiecke, S. Will, P. Ahmadi, and M. W. Zwierlein, *Phys. Rev. A* **85**, 051602(R) (2012).
- [25] J. Ulmanis, S. Häfner, R. Pires, E. D. Kuhnle, M. Weidemüller, and E. Tiemann, *New J. Phys.* **17**, 055009 (2015).
- [26] Z. Fu, L. Huang, Z. Meng, P. Wang, L. Zhang, S. Zhang, H. Zhai, P. Zhang, and J. Zhang, *Nat. Phys.* **10**, 110 (2014).
- [27] H. Yang, D.-C. Zhang, L. Liu, Y.-X. Liu, J. Nan, B. Zhao, and J.-W. Pan, *Science* **363**, 261 (2019).
- [28] C. Chin and P. S. Julienne, *Phys. Rev. A* **71**, 012713 (2005).
- [29] E. Braaten, H. W. Hammer, D. Kang, and L. Platter, *Phys. Rev. A* **81**, 013605 (2010).
- [30] K. Helfrich, H.-W. Hammer, and D. S. Petrov, *Phys. Rev. A* **81**, 042715 (2010).
- [31] C. Gao and P. Zhang, *Phys. Rev. A* **97**, 042701 (2018).